Available online at www.sciencedirect.com
SCIENCE DIRECT®
Talanta 66 (2005) 943–951
Talanta
www.elsevier.com/locate/talanta

Extraction of cationic surfactant templates from mesoporous materials by CH_3OH-modified CO_2 supercritical fluid

L. Huang[a,*], S. Kawi[b], C. Poh[b], K. Hidajat[b], S.C. Ng[c]

[a] *Institute of Chemical and Engineering Sciences, 1 Pesek Road, Jurong Island, Singapore 627833, Singapore*
[b] *Department of Chemical and Biomolecular Engineering, National University of Singapore, Singapore 117576, Singapore*
[c] *Department of Chemistry, National University of Singapore, Singapore 117543, Singapore*

Received 3 September 2004; received in revised form 17 December 2004; accepted 17 December 2004
Available online 30 January 2005

Abstract

Extraction of cationic surfactant templates from MCM-41, MCM-48, SBA-1 and SBA-3 has been conducted using CH_3OH-modified CO_2 supercritical fluid. The supercritical fluid extraction (SFE) has been integrated with thermogravimetry (TG), X-ray diffraction (XRD) and N_2 adsorption–desorption to evaluate extraction efficiency and structural stability of mesoporous materials. Experiments of optimization indicate that the conditions of 90 bar, 85 °C, CH_3OH/CO_2 = 0.1/1.0 ml/min and 3 h are most suitable for the SFE of cationic templates. 76–95% of the cationic templates can be extracted from the mesoporous materials. XRD and N_2 adsorption–desorption studies illustrate that SFE possesses some advantages over calcination in maintaining mesoporous uniformity and structural stability when used to remove templates. The impact of curing on mesoporous structure is also dealt with.

Keywords: Supercritical fluid extraction; Cationic; Template; Mesoporous materials

1. Introduction

Mesoporous materials are referred to as promising materials applied to adsorption, catalysis and separation, etc., owing to an arrangement of uniform-sized mesopores (15–50 Å) and a high surface area (>700 m^2/g). Currently, M41S and SBA families represent two important types of mesoporous materials. The synthesis of MCM-41 (hexagonal *p*6*m*), MCM-48 (cubic *Ia*3*d*), SBA-1 (cubic *Pm*3*n*) and SBA-3 (hexagonal *p*6*m*) makes use of cationic organic surfactants as the templates or structure-directing agents. In the structures of these as-synthesized mesoporous materials, there is an electrostatic S^+I^- interaction between the aliphatic groups of the surfactant and the siliceous oligomers and thereby the surfactant is strongly bonded to the silicate unit [1]. It is difficult to recover the surfactant from the organic/inorganic ion pair packing by extraction with a simple polar solvent [1,2].

To make mesoporous materials function as adsorbents, catalysts and membranes and so on, a large amount of organic template must be removed from the pores so as to render them accessible. It is known that the removal of organic templates usually is difficult unless they are destroyed and that the costs of organic templates in many instances occupy a major proportion in the total costs of mesoporous materials [2]. For example, the organic template cetyltrimethylammonium bromide (CTMABr) constitutes approximately 77% of the material cost for the manufacture of silicate MCM-41. Apparently, template removal would better combine with their recovery, by which the cost of manufacture of mesoporous materials can greatly be reduced.

A number of methods for removing organic templates have been documented, including calcination, ozone treatment, solvent extraction and SFE [1–6]. Calcination is most commonly used to burn off organic templates at high

* Corresponding author. Tel.: +65 67963831; fax: +65 63166182.
E-mail address: huanglin1@yahoo.com (L. Huang).

0039-9140/$ – see front matter © 2005 Elsevier B.V. All rights reserved.
doi:10.1016/j.talanta.2004.12.057

temperatures (540–600 °C). Although organic templates can completely be removed, calcination has some drawbacks. It does not allow the recovery of expensive organic templates. Emitted noxious gases during the calcination process lead to environmental pollution. It is a time-consuming process, which requires at least 10 h for completion excluding the temperature build-up time. What is more, it causes the condensation of silanol groups in the mesopores to form siloxane bonds at high temperatures, thus resulting in a lowering of *d*-values or pore contraction [7–9].

Ozone treatment enables full oxidation of organic templates in the mesopores at temperatures not exceeding 250 °C and thus maintains the structures of final mesoporous materials unchanged [4,10,11]. Although complete removal of organic templates can be reached, they cannot be recovered, either, and toxic gases formed still pollute the atmosphere.

Solvent extraction is an alternative approach to template removal [1,2]. Quantitative extraction of nonionic templates from mesoporous materials can utilize a pure organic solvent [1,12,13]. Using a liquid mixture comprising of at least one polar solvent and at least one cation donor, cationic templates can efficiently be extracted from mesoporous materials at temperatures between 50 and 100 °C [2,7,14–18]. The extracted cationic templates can quantitatively be recovered without loss of quality. But a huge amount of liquid solvent is necessary, which results in a dilute extract and makes eventual solvent disposal a rather challenging step. The extraction processes require several hours or even days to perform. After extraction, it has been reported that the crystallinity of final mesoporous materials are reduced in some cases [14,16,18].

Supercritical fluids possess unique physicochemical properties that make them attractive as extraction solvents. The combined gas-like mass transfer and liquid-like solvating characteristics have led to considerable excitement for their use as mobile phases to extract analysts [19,20]. Supercritical CO_2 has been the most widely used extraction fluid because of low critical point at 31.1 °C and 72.8 bar, low cost, and low toxicity and reactivity [19,20]. Since the low polarity of CO_2 limits its use to the extraction of relatively apolar or moderately polar analysts, a small amount of a polar organic modifier has been added to supercritical CO_2 for the extraction of polar analysts. The modified supercritical CO_2 has widely been used to solvate organic compounds and extract analysts from the matrix by interrupting analyst–matrix interactions [6,13,20–30]. This method is expected to yield rapidly quantitative recovery of target analysts. SFE has obvious advantages over solvent extraction: it is fast and generally is complete in 10–60 min; the separation steps of extracts are greatly simplified with supercritical CO_2; the amount of solvent used is considerably reduced with SFE.

In this paper, we shall report a detail study of CH_3OH-modified CO_2 SFE of CTMABr from MCM-48. We also shall describe the results of extended studies on MCM-41, SBA-1 and SBA-3. The work presented here includes relevant analysis and structural characterization of the mesoporous materials studied by means of TG, XRD and N_2 adsorption–desorption.

2. Experimental

Sodium silicate solution (25.5–28.5% SiO_2, 7.5–8.5% Na_2O) and CTMABr (98–101%) were purchased from Merck. Tetraethyl orthosilicate (TEOS, 98%) and triethylamine (99%) were obtained from Aldrich. Cetyltriethylammonium chloride (CTMACl, 25% in aqueous solution) and 1-bromohexadecane (97%) were supplied by Acros. All other reagents were purchased commercially.

Silicate MCM-41 was synthesized as described in Ref. [31]. After hydrothermal reaction, the solid was filtered off, washed with deionized water until free of Br^- and dried under vacuum at room temperature.

Silicate MCM-48 was synthesized using a molar composition of gel of 1.0TEOS:0.65CTMABr:0.50NaOH:62H_2O. 1.09 g of NaOH and 56 ml of deionized water were added to 12.00 g of CTMABr. After the solution had been stirred for 10 min, 11.2 ml of TEOS was poured to form a gel. The gel mixture was stirred for 1.5 h, transferred into a polypropylene bottle and heated in an oven at 100 °C for 4 days under autogenerated pressure. After hydrothermal treatment, the powder was filtered off, washed with deionized water until free of Br^- and dried under vacuum at room temperature.

Silicate SBA-1 was synthesized according to the method reported by Kim and Ryoo [32]. Cetyltriethylammonium bromide (CTEABr) was obtained by action of 1-bromohexadecane with equimolar triethylamine followed by recrystallization [32]. 1.5 g of CTEABr, 85.75 ml of HCl (37%) and 168.50 ml of deionized water were combined to give a homogeneous surfactant solution, which was then cooled using an ice bath. 4.15 ml of TEOS was precooled and added to the above cooled solution under vigorous stirring. The resulting gel had a molar composition of 1.0CTEABr:5.0TEOS:280HCl:3500H_2O. Stirring was continued for 4 h until the precipitation of the silica–surfactant assemblies was completed. Then the reaction mixture was heated to 100 °C rapidly and treated at 100 °C for 1 h. The resulting precipitate was filtered off and dried in an oven at 100 °C overnight.

Silicate SBA-3 was synthesized referring to the method reported by Huo et al. [33]. 6.0 g of CTMABr, 104.80 ml of HCl (37%) and 242.75 ml of deionized water were combined to obtain a homogeneous surfactant solution. 30.50 ml of TEOS was added to the solution under vigorous stirring. The resulting gel had a molar composition of 1.0CTMABr:3.8TEOS:77HCl:1095H_2O. Stirring was continued for 4 h until the precipitation of the silica–surfactant assemblies was completed. The resulting precipitate was filtered off and dried in an oven at 100 °C overnight.

In order to improve cross-linking of the silicate framework, part of each as-synthesized mesoporous material was

cured at 160 °C under vacuum for 14 h. Although C_{16}TABr is known to start to decompose at around 150 °C and be completely removed from mesostructured silica at around 400 °C in air [7,14,34,35], the template weights were not lost after as-synthesized mesoporous materials had been cured under vacuum for 14 h. Identical TG curves were observed for as-synthesized and cured samples of each material.

Experiments of SFE of templates were conducted on a Jasco SFE apparatus. This apparatus consists of a cylinder of highly pure CO_2, a HPLC pump for CO_2, a syringe pump for modifier, a chiller, a 10-ml extraction vessel, an oven and a pressure restrictor. A sample of 0.5 g was placed in the extraction vessel. The chiller temperature was set to approximately −5 °C to ensure that CO_2 could be chilled to a liquid phase, thus preventing cavitation of the CO_2 pump. The desired temperature and pressure were set on the oven and the pressure restrictor, respectively. The flow rate of CO_2 was set at 1.0 ml/min.

Once the desired pressure reached, the modifier pump was turned on and dynamic extraction with continuous injection of the modifier was performed under the desired conditions. The extracted template together with the modifier was collected in a vial at the outlet of backpressure regular. After extraction, the sample in the extraction vessel was dried at 80 °C before analysis and characterization.

Experiments of CH_3OH extraction were performed by refluxing 0.5 g of as-synthesized sample with 100 ml of CH_3OH under atmospheric pressure for 3 h. After extraction, the sample was filtered off, washed with 50 ml of CH_3OH and dried at 80 °C before analysis.

Experiments of sample calcination to burn off templates were carried out using a furnace by programmed heating at 0.2 °C/min from 23 to 540 °C followed by 24 h of isothermic heating at 540 °C.

The amounts of templates in the samples were determined by TG on a Shimadzu DTG-50 thermogravimetric analyzer. The samples were heated to 600 °C at 10 °C/min in air. The extraction efficiency was estimated by comparing the amount of template remaining on the sample after SFE or CH_3OH extraction with the amount of template on the as-synthesized sample.

XRD of the samples was performed on a Shimadzu XRD-6000 spectrometer with Cu Kα monochromatic radiation. N_2 adsorption–desorption of the samples after template removal was measured on a Quantachrome Autosorb-1 analyzer.

3. Results and discussion

3.1. Optimization of SFE conditions

The experimental conditions for performing CO_2 SFE of cationic templates were optimized with cured MCM-48 with regard to modifier concentration, extraction time, extraction temperature and extraction pressure. First of all, the SFE result with CO_2 alone showed that no CTMABr is extracted from cured MCM-48 over wide ranges of temperatures (85 and 120 °C) and pressures (90 and 350 bar). This confirms that the polarity of CO_2 is too low to be able to extract the ionic compound bonded chemically to the matrix [19,20]. Hence, supercritical CO_2 must be combined with a polar modifier to increase the solvating power toward $CTMA^+$ occluded within MCM-48.

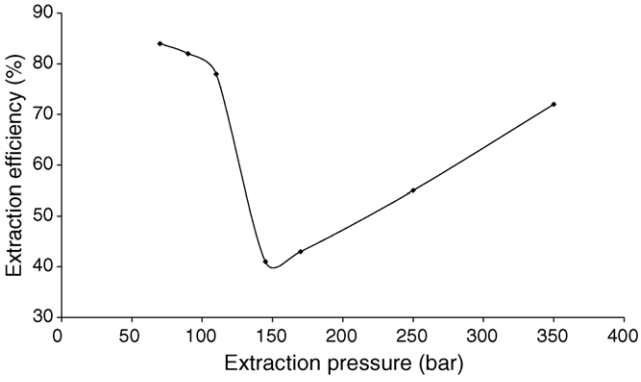

Fig. 1. Extraction efficiency of CTMABr from cured MCM-48 as a function of pressure at 85 °C with CH_3OH/CO_2 (0.1/1.0 ml/min) for 3 h.

CH_3OH is an excellent choice as an effective modifier based on available data in the literature [20]. Since CO_2/CH_3OH binary mixtures are in a supercritical state at pressures above 165 bar and at temperatures below 100 °C [33], the effect of CH_3OH concentration on the SFE efficiency was examined at 85 °C and 350 bar. As a result, the SFE efficiency of CTMABr increased significantly with increasing CH_3OH flow rate up to 76% at 0.1 ml/min. From above 0.1 ml/min, the efficiency did increase quite slowly. This indicates that adding CH_3OH does greatly enhance the extraction efficiency of CTMABr and that the optimal CH_3OH flow rate is 0.1 ml/min for a CO_2 flow rate of 1.0 ml/min.

Fig. 1 shows the extraction efficiency of CTMABr as a function of pressure between 70 and 350 bar at 85 °C with CH_3OH/CO_2 (0.1/1.0 ml/min). Between 70 and 150 bar, the extraction efficiency decreased with pressure, while between 150 and 350 bar, it increased with pressure. The increase in extraction efficiency above 150 bar can be understood in terms of the increase in the supercritical fluid density with increasing pressure [20], because a CO_2/CH_3OH mixture exists in a supercritical liquid phase at 85 °C and above 141 bar [36]. The increase in supercritical fluid density leads to an increase in solvating ability. However, the decrease in extraction efficiency between 70 and 150 bar cannot be explained by the variation of solubility of the single liquid phase with pressure, because the CO_2/CH_3OH mixture exists in both liquid and vapor phases in the conditions. Such extraction proceeds actually in a subcritical state. The CH_3OH may be entrained as liquid droplets in the gaseous CO_2 when passing through the sample matrix. The CO_2 plays the role of a carrier gas. At a lower pressure, a smaller CO_2 density produced can help the CH_3OH enter the pores of MCM-48 to dissolve CTMABr,

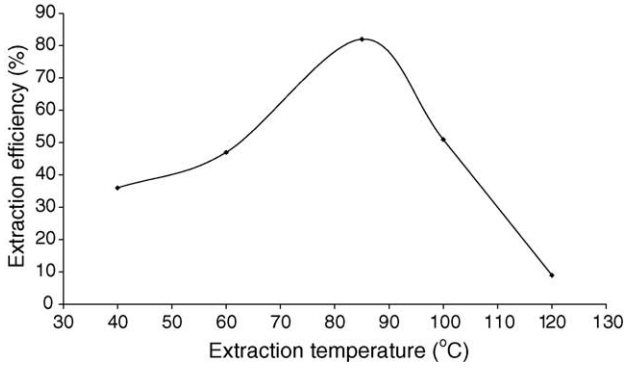

Fig. 2. Extraction efficiency of CTMABr from cured MCM-48 as a function of temperature at 90 bar with CH_3OH/CO_2 (0.1/1.0 ml/min) for 3 h.

a lower CO_2 viscosity obtained can favor the diffusion of the CH_3OH in and out of the pores of MCM-48. Therefore, higher extraction of CTMABr is obtained at a lower pressure in this subcritical region. It was noted that extraction at 70–100 bar which yielded 80–84% of CTMABr is even more efficient than SFE at 350 bar.

Fig. 2 shows the extraction efficiency of CTMABr as a function of temperature at 90 bar with CH_3OH/CO_2 (0.1/1.0 ml/min). The extraction efficiency grew as the temperature increased up to a maximum of 82% and then fell rapidly. Since CTMABr is an ionic solute, it is strongly attached to the channel walls of MCM-48 via electrostatic interaction. Its removal from the matrix must overcome an energy barrier of chemical desorption.

Accordingly, increasing the temperature up to 85 °C can accelerate the chemical desorption of CTMABr and thereby enhance the extraction efficiency. From above 85 °C, the decrease in extraction efficiency may be related to the decreased solubility of CTMABr in CO_2/CH_3OH with temperature. The solubility of CTMABr in CO_2/CH_3OH seems to be the limiting factor that increases the extraction efficiency at higher temperatures. The results are consistent with those reported previously for SFE of target analysts from the matrix that have the same trend [6,22].

From the above observations on the influences of extraction temperature and extraction pressure on the extraction efficiency of CTMABr from MCM-48 with CO_2/CH_3OH, 85 °C and 90 bar were recommended to be the most appropriate extraction temperature and pressure in the title work. An optimal extraction time of 3 h was found out from the extraction results using these experimental conditions.

3.2. Studies on SFE of cationic templates from various mesoporous materials

In the light of the optimal experimental conditions established with cured MCM-48, we extended the SFE investigation of cationic templates to MCM-41, SBA-1 and SBA-3. SFE efficiencies on as-synthesized and cured samples were compared. SFE data were combined with XRD spectra and N_2 adsorption–desorption results of the samples to reveal the structural evolution of mesoporous materials during the SFE and to demonstrate the effects of curing on the structural stability of mesoporous materials. In Table 1 are presented the template extraction efficiencies, physical properties and structural stability of MCM-41, MCM-48, SBA-1 and SBA-3. In Table 2 are shown the XRD information of these materials before and after template removal.

Table 1
Template removal results, physical properties and structural stability of various mesoporous materials

Material	SFE efficiency (%)	CH_3OH extraction efficiency (%)	Mean pore diameter (Å)	Total pore volume (cm^3/g)	BET surface area (m^2/g)	Structure after template removal
As-synth. MCM-41[a]	78		29.2	0.81	1332	Stable
As-synth MCM-41[b]		28				
As-synth. MCM-41[c]			30.5	1.29	1651	Stable
Cured MCM-41[a]	76		27.9	0.78	1250	Stable
As-synth. MCM-48[a]	93		–	–	–	Destroyed
As-synth MCM-48[b]		20				
As-synth. MCM-48[c]			26.3	0.81	1225	Stable
Cured MCM-48[a]	82		23.6	0.82	1411	Stable
Cured MCM-48[c]			23.5	0.86	1412	Stable
As-synth. SBA-1[a]	88		23.4	1.34	2447	Stable
As-synth SBA-1[b]		22				
As-synth. SBA-1[c]			21.8	1.06	2057	Stable
Cured SBA-1[a]	87		22.5	1.09	2086	Stable
Cured SBA-1[c]			22.0	0.69	1298	Stable
As-synth. SBA-3[a]	95		–	–	–	Destroyed
As-synth SBA-3[b]		26				
As-synth. SBA-3[c]			18.5	0.89	1686	Stable
Cured SBA-3[a]	85		22.5	1.09	2152	Stable
Cured SBA-3[c]			19.1	0.58	1052	Stable

[a] Template removal by SFE under the conditions of 85 °C, 90 bar, CH_3OH/CO_2 = 0.1/1.0 ml/min, 3 h and 0.5 g of sample.
[b] Template removal by CH_3OH extraction under reflux at atmospheric pressure with 0.5 g of sample and 100 ml of CH_3OH.
[c] Template removal by calcination at 540 °C.

Table 2
XRD peak positions in the 1.5–10° 2θ range of various mesoporous materials

	MCM-41	MCM-48	SBA-1	SBA-3
As-synthesized				
Before template removal	2.02, 3.60, 4.08	2.20, 2.54, 4.26	2.06, 2.32, 2.48, 3.78	2.32, 4.10, 4.76
After SFE	2.08, 3.64, 4.20	None	2.08, 2.30, 2.52, 3.88	None
After calcination	2.10, 3.74, 4.34	2.48, 2.88, 4.66	2.16, 2.40, 2.64, 3.82	2.80, 4.96, 5.96
Cured				
Before template removal	2.12, 3.72, 4.34	2.54, 2.90, 4.86	2.06, 2.28, 2.50, 3.84	2.42, 4.24
After SFE	2.16, 3.76, 4.36	2.48, 2.88, 4.68	2.16, 2.32, 2.54, 3.86	2.48, 4.28, 4.96
After calcination	2.18, 3.78, 4.38	2.56, 2.94, 4.94	2.24, 2.50, 2.74, 4.08	2.88, 4.94, 5.92

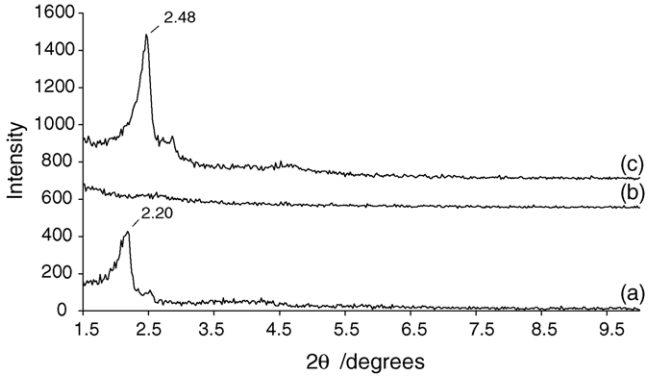

Fig. 3. XRD patterns of (a) as-synthesized MCM-48; (b) as-synthesized MCM-48 after 3 h of template SFE; (c) as-synthesized MCM-48 after calcination.

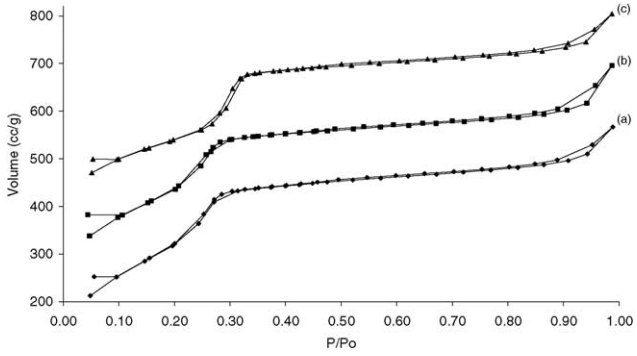

Fig. 5. N_2 adsorption–desorption isotherms of (a) cured MCM-48 after 6 h of template SFE; (b) cured MCM-48 after calcination; (c) as-synthesized MCM-48 after calcination.

In the case of MCM-48, 93% and 82% represent significant SFE efficiencies of CTMABr from as-synthesized MCM-48 and from cured MCM-48, respectively. Although the template extraction is more complete on as-synthesized MCM-48 than on cured MCM-48, the mesoporous structure of as-synthesized MCM-48 is fully destroyed and that of cured MCM-48 is retained during the SFE. As a matter of fact, the diffraction peaks for MCM-48 disappeared thoroughly after 3 h of SFE on as-synthesized MCM-48, taking a look at a set of relevant XRD spectra shown in Fig. 3. In contrast, the diffraction peak intensities after 6 h of SFE on cured MCM-48 were comparable to those after template removal on MCM-48 by calcination, as shown in Figs. 3 and 4. This accounts for that template removal on cured MCM-48 via SFE produces a similar mesoporous structural ordering to that via calcination. Moreover, a type IV N_2 adsorption–desorption isotherm with a narrow pore size distribution was maintained after 6 h of SFE on cured MCM-48, which was identical with that after calcination on cured MCM-48, as seen in Figs. 5 and 6.

It was surprisingly noticed that curing treatment of as-synthesized MCM-48 at 160 °C already led to marked shift of peaks to higher 2θ angles in addition to decreased peak intensity in XRD, as seen in Fig. 4(a) and (b). The intensity decrease of diffraction peaks suggests the lowering of

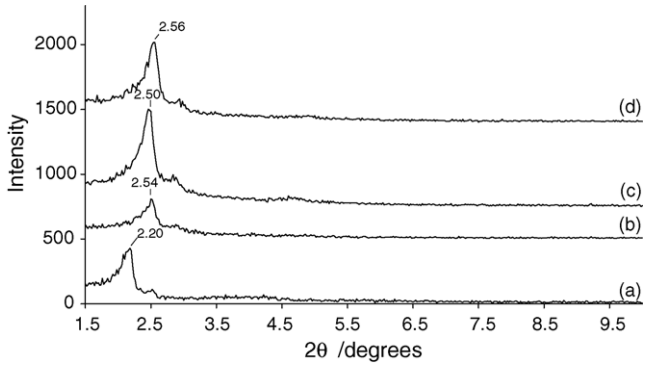

Fig. 4. XRD patterns of (a) as-synthesized MCM-48; (b) cured MCM-48; (c) cured MCM-48 after 6 h of template SFE; (d) cured MCM-48 after calcination.

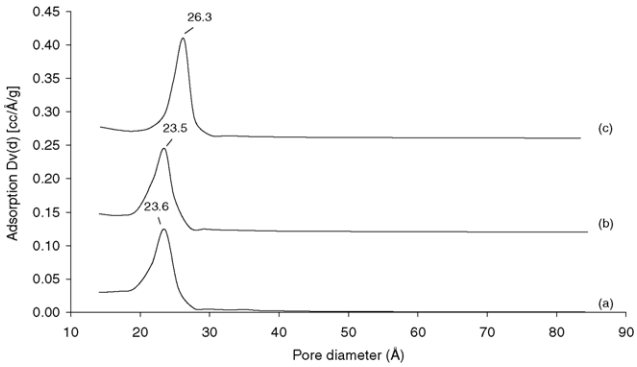

Fig. 6. Pore size distributions of (a) cured MCM-48 after 6 h of template SFE; (b) cured MCM-48 after calcination; (c) as-synthesized MCM-48 after calcination.

mesopore uniformity. The upward shift of diffraction peaks, namely the lowering of *d*-values implies the occurrence of mesopore contraction. The shift value was slightly higher than that after calcination on as-synthesized MCM-48. The N_2 adsorption–desorption isotherms of cured MCM-48 showed capillary condensation steps at low relative pressures, compared to the case of as-synthesized MCM-48 by calcination. The corresponding mean pore diameters (∼24 Å) were smaller than that of as-synthesized MCM-48 after calcination (∼26 Å). These indicate more severe pore contraction for cured MCM-48 than for as-synthesized MCM-48, in accordance with XRD data. In spite of the bigger structural shrinkage and decreased structural ordering, cured MCM-48 can remain structurally stable under SFE conditions. There were no significant changes in XRD peak position and in N_2 adsorption–desorption after template removal by SFE and by calcination. In total pore volume and in BET surface area, removing the template via SFE led to almost no changes and curing as-synthesized MCM-48 only resulted in slight changes, as indicated in Table 1. It is evident that the fragility of as-synthesized MCM-48 structure can be improved by reinforcing cross-linking of the silicate framework via curing.

In the case of MCM-41, close SFE efficiencies of CTMABr of 78% and 76% were achieved from as-synthesized MCM-41 and from cured MCM-41. The diffraction peaks after 6 h of SFE on as-synthesized MCM-41 were similar to those after template removal on as-synthesized MCM-41 by calcination. This implies that as-synthesized MCM-41 is stable under SFE conditions and quite ordered after template SFE in structure. Curing as-synthesized MCM-41 led to a slight upward shift in diffraction peak position and a marked increase in diffraction peak intensity. The upward shift is comparable to that caused by calcination on as-synthesized MCM-41. The intensity increase suggests the improvement of mesopore uniformity. The subsequent template removal by SFE and by calcination further little the upward shift. But the diffraction peak intensities after 6 h of SFE on cured MCM-41 were significantly higher than those after template removal on cured MCM-41 by calcination. This indicates that template removal via SFE brings about a higher structural ordering than template removal via calcination on cured MCM-41. It was also noted that after template SFE the diffraction peak intensities were comparable on cured MCM-41 and on as-synthesized MCM-41, accounting for their consistency in structural property.

N_2 adsorption–desorption indicated that after 6 h of SFE as-synthesized MCM-41 and cured MCM-41 had similar type IV adsorption–desorption isotherms (Fig. 7) which were accompanied by similar pore size distributions. Their capillary condensation steps appeared at lower relative pressures than those at which the capillary condensation step of as-synthesized MCM-41 after template removal by calcination arose. Compared to the case of as-synthesized MCM-41 after template removal by calcination, their

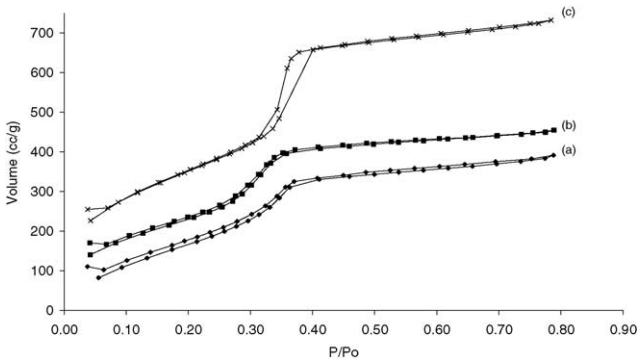

Fig. 7. N_2 adsorption–desorption isotherms of (a) as-synthesized MCM-41 after 6 h of template SFE; (b) cured MCM-41 after 6 h of template SFE; (c) as-synthesized MCM-41 after calcination.

capillary condensation step heights and mean pore diameters were small. These may be due to irregular pore filling with the remaining template in important amounts (22–24%). After SFE, cured MCM-41 displayed a slightly smaller mean pore diameter than as-synthesized MCM-41 in agreement with XRD study. Consistently, SFE-treated MCM-41 had smaller total pore volumes and BET surface areas than calcined MCM-41, and curing as-synthesized MCM-41 only led to weak decreases in total pore volume and in BET surface area (Table 1).

These results illustrate that SFE is effective for the template removal from MCM-41 without the structural degradation of MCM-41 and that curing causes a negligible depletion in the structure and physical properties of MCM-41.

In the case of SBA-1, as-synthesized SBA-1 and cured SBA-1 gave close SFE efficiencies of CTEABr of 88% and 87%. Figs. 8 and 9 show the XRD patterns collected during the SFE of CTEABr on SBA-1. For as-synthesized SBA-1, the diffraction spectral intensity grew notably with extraction time. This demonstrates that the mesoporous structure of as-synthesized SBA-1 becomes more and more ordered as the template is extracted. From after 3 h, the intensity was found to exceed that of calcined SBA-1. Comparatively, the intensity did not change after template extraction for cured

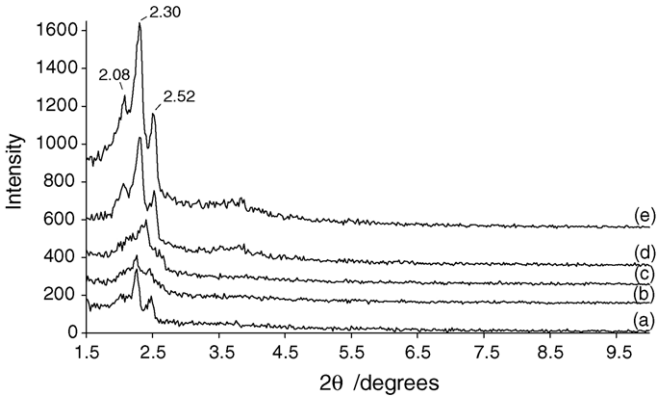

Fig. 8. XRD patterns of as-synthesized SBA-1 after template SFE for (a) 0 h; (b) 0.5 h; (c) 1 h; (d) 3 h; (e) 6 h.

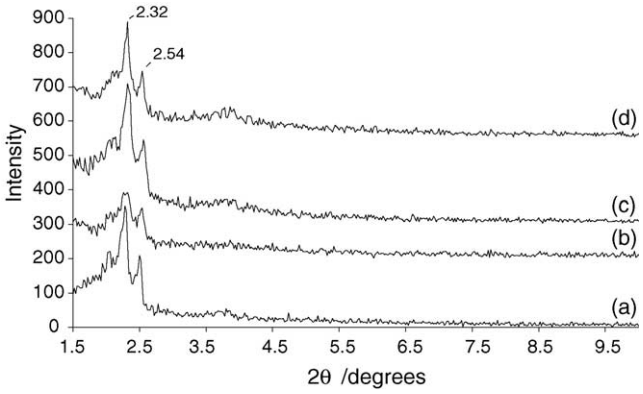

Fig. 9. XRD patterns of cured SBA-1 after template SFE for (a) 0 h; (b) 1 h; (c) 3 h; (d) 6 h.

SBA-1 (Fig. 9). Moreover curing as-synthesized SBA-1 altered the diffraction spectrum of as-synthesized SBA-1 in both position and intensity only to a small extent. These suggest that curing and subsequent SFE affect little the mesoporous structural ordering of as-synthesized SBA-1. For both as-synthesized SBA-1 and cured SBA-1, SFE of template did not cause any diffraction peak shift, differing from calcination of template which resulted in apparent upward shift of diffraction peak positions due to pore contraction. Cured SBA-1 after calcination showed bigger upward shift than as-synthesized SBA-1 after calcination, proposing the positive effect of curing on the pore contraction of SBA-1.

Fig. 10 shows the N_2 adsorption–desorption isotherms of related SBA-1 samples. Consistent with the XRD observations, the extracted samples gave capillary condensation steps at slightly higher relative pressures than those at which the calcined samples did, and greater mean pore diameters than the calcined samples. The results confirm that template removal by SFE can keep SBA-1 from pore contraction. For the calcined cured sample, there is a loss of capillary condensation step concomitant with a broadening of pore size distribution. This is indicative of the depletion of mesopore uniformity of cured SBA-1 by calcination. In agreement with XRD study, a cured sample had a slightly

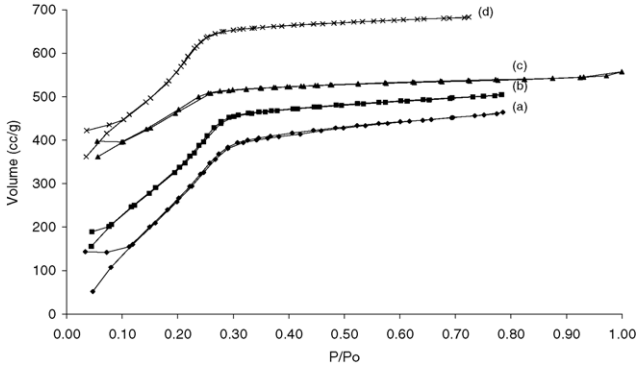

Fig. 10. N_2 adsorption–desorption isotherms of (a) as-synthesized SBA-1 after 6 h of template SFE; (b) cured SBA-1 after 6 h of template SFE; (c) cured SBA-1 after calcination; (d) as-synthesized SBA-1 after calcination.

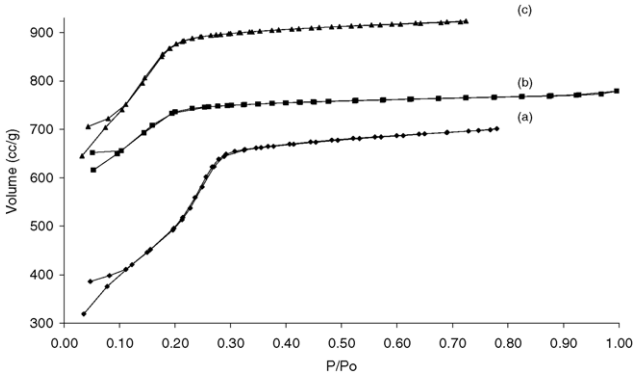

Fig. 11. N_2 adsorption–desorption isotherms of (a) cured SBA-3 after 12 h of template SFE; (b) cured SBA-3 after calcination; (c) as-synthesized SBA-3 after calcination.

smaller mean pore diameter than a related as-synthesized sample because of weak pore contraction. At the same time, the total pore volumes and BET surface areas of the extracted samples were consistently markedly greater than those of the calcined samples, and curing as-synthesized SBA-1 consistently led to significant systematic decreases in total pore volume and in BET surface area (Table 1).

According to these data, it is reasonably assumed that SFE of template not only hardly reduces the pore size of SBA-1 but also improves the structural ordering of as-synthesized SBA-1, and that curing as-synthesized SBA-1 decreases the total pore volume and BET surface area of SBA-1.

In the case of SBA-3, the extraction efficiencies of CTMABr amounted to 95% on as-synthesized SBA-3 and to 85% on cured SBA-3, which made a significant difference. Nevertheless, the structure of as-synthesized SBA-3 collapsed completely and the structure of cured SBA-3 fairly remained during the SFE, as evidenced by related XRD spectra. Furthermore, curing as-synthesized SBA-3 only led to slight upward shift in diffraction peak position and slight decrease in diffraction peak intensity. The subsequent SFE enhanced considerably the intensity although it merely increased slightly the upward position shift. The resulting intensity after SFE was superior to those observed after calcination on SBA-3. This shows that cured SBA-3 after template removal via SFE is more ordered in structure than SBA-3 after template removal via calcination. In contrast, a great upward position shift occurred when template removal was carried out by calcination on either as-synthesized SBA-3 or cured SBA-3. This is ascribed to heavy pore contraction of SBA-3 upon calcination.

On the N_2 adsorption–desorption isotherms, only cured SBA-3 after SFE maintained a type IV shape and SBA-3 after calcination lost apparently the capillary condensation step, as presented in Fig. 11. On the pore size distributions, only cured SBA-3 after SFE displayed a narrow peak and SBA-3 after calcination gave broad peaks. The mean pore diameter of cured SBA-3 after SFE was much greater than those of SBA-3 after calcination. In the meantime, the total pore volume and BET surface area of the former were much

greater than those of the latter, and curing as-synthesized SBA-3 caused marked decreases in total pore volume and in BET surface area (Table 1). These agree with the results by XRD, demonstrating the good mesopore uniformity of cured SBA-3 after SFE and the ill mesopore uniformity and serious pore contraction of SBA-3 after calcination.

Accordingly, the template elimination of SBA-3 behaves a little like that of MCM-48. The structure of as-synthesized SBA-3 is too fragile to withstand the SFE conditions of template. Curing enables stabilization of the SBA-3 structure and prevention of its collapse during the SFE. Besides, the SFE of template on cured SBA-3 can ensure the achievement of uniform SBA-3 mesoporous structures, which the calcination method cannot.

Finally, it is clearly seen from Table 1 that SFE with CO_2/CH_3OH has the incomparable advantage of securing high template extraction efficiencies over solvent extraction with CH_3OH. Only 20–28% of the templates was extracted from the mesoporous materials via the latter, consistent with low efficiencies reported for the cationic template extractions from MCM-41 and MCM-48 with C_2H_5OH under equivalent conditions [15,17]. Such a difference than the former in extraction efficiency lies in the limited solubility of the templates in CH_3OH and in the difficulty surmounting the electrostatic interaction of cationic templates with channel walls of mesostructured silica by CH_3OH extraction.

4. Conclusions

This work has involved the exploration of CH_3OH-modified CO_2 SFE of a cationic surfactant template on MCM-48 and the investigation of cationic template removal on MCM-41, MCM-48, SBA-1 and SBA-3 in connection with their physical and structural properties. The optimal conditions of 90 bar, 85 °C, CH_3OH/CO_2 = 0.1/1.0 ml/min and 3 h are proposed to be applied to the SFE of templates from these mesoporous materials. SFE efficiencies of 76–95% are obtained on these materials. Generally, SFE is of marked advantages over calcination for template removal in obtaining the high structural ordering and good structural stability of mesoporous materials. For MCM-41 and SBA-1, as-synthesized materials substantially remain structurally stable throughout the SFE processes. It is not recommended to cure the as-synthesized materials in improving the performances of ultimate mesoporous materials. SFE of template directly from as-synthesized SBA-1 evidently favors increasing the structural ordering of SBA-1 as well as avoiding the pore contraction and the reduction of pore volume and surface area of SBA-1. For MCM-48 and SBA-3, as-synthesized materials collapse readily in structure upon template removal by SFE. It is necessary to cure the as-synthesized materials for stabilizing their ordered structures and thus preventing the structural destruction under SFE conditions. Interestingly, the uniform SBA-3 mesopores are achieved only by SFE of template from cured SBA-3. In addition, it appears that template removal by calcination could produce uniform mesopores for MCM-41 and MCM-48 and could hardly for SBA-1 and SBA-3. Since the materials studied possess distinct mesoporous structures and physical properties that are embodied in the different behaviors during the template removal, it is difficult to draw a general trend relating to the synthetic conditions or porous structure based on the present work.

Acknowledgments

This research project was financially supported by ABB Lummus Global, Inc. The authors thank Prof. Frits M. Dautzenberg for helpful discussion and information.

References

[1] P.T. Tanev, T.J. Pinnavaia, Science 267 (1995) 865.
[2] D.D. Whitehurst, U.S. Patent 5,143,879 (1992).
[3] C.T. Kresge, M.E. Leonowicz, W.J. Roth, J.C. Vartuli, J.S. Beck, Nature 359 (1992) 710.
[4] M.T.J. Keene, R. Denoyed, P.L. Llewellyn, Chem. Commun. (1998) 2203.
[5] A. Hozumi, H. Sugimura, K. Hiraku, T. Kameyama, O. Takai, Chem. Mater. 12 (2000) 3842.
[6] S. Kawi, M.W. Lai, AIChE J. 48 (2002) 1572.
[7] C.-Y. Chen, H.-X. Li, M.E. Davis, Micropor. Mater. 2 (1993) 17.
[8] J.M. Kim, S.K. Kim, R. Ryoo, Chem. Commun. (1998) 259.
[9] K. Schumacher, M. Grün, K.K. Unger, Micropor. Mesopor. Mater. 27 (1999) 201.
[10] T. Clark Jr., J.D. Ruiz, H. Fan, C.J. Brinker, B.I. Swanson, A.N. Parikh, Chem. Mater. 12 (2000) 3879.
[11] G. Büchel, R. Denoyel, P.L. Llewellyn, J. Rouquerol, J. Mater. Chem. 11 (2001) 589.
[12] A.G.S. Prado, C. Airoldi, J. Mater. Chem. 12 (2002) 3823.
[13] R. van Grieken, G. Calleja, G.D. Stucky, J.A. Melero, R.A. García, J. Iglesias, Langmuir 19 (2003) 3966.
[14] R. Schmidt, D. Akporiaye, M. Stöcker, O.H. Ellestad, Stud. Surf. Sci. Catal. 84 (1994) 61.
[15] S. Hitz, R. Prins, J. Catal. 168 (1997) 194.
[16] Z.-L. Hua, J.-L. Shi, L. Wang, W.-H. Zhang, J. Non-Cryst. Solids 292 (2001) 177.
[17] M. Benjelloun, P. van Der Voort, P. Cool, O. Collart, E.F. Vansant, Phys. Chem. Chem. Phys. 3 (2001) 127.
[18] A. Doyle, B.K. Hodnett, Micropor. Mesopor. Mater. 58 (2003) 255.
[19] S.B. Hawthorne, Anal. Chem. 62 (1990) 633.
[20] V. Camel, A. Tambuté, M. Caude, J. Chromatogr. 642 (1993) 263, and references therein.
[21] T.S. Reighard, S.V. Olesik, J. Chromatogr. A 737 (1996) 233.
[22] X. Lou, H.-G. Janssen, C.A. Cramers, J. Chromatogr. Sci. 34 (1996) 282.
[23] J. Pörschmann, L. Blasberg, K. Mackenzie, P. Harting, J. Chromatogr. A 816 (1998) 221.
[24] C. Danumah, S.M.J. Zaidi, N. Voyer, S. Giasson, S. Kaliaguine, Stud. Surf. Sci. Catal. 117 (1998) 281.
[25] D. Pyo, H. Shin, Anal. Chem. 71 (1999) 4772.
[26] Y.S. Fung, Y.H. Long, J. Chromatogr. A 907 (2001) 301.
[27] Y.-C. Sun, Y.-T. Chung, J. Mierzwa, Analyst 126 (2001) 1694.
[28] P. Kluson, P. Kacer, T. Cajthaml, M. Kalaji, J. Mater. Chem. 11 (2001) 644.
[29] X.-B. Lu, W.-H. Zhang, J.-H. Xiu, R. He, L.-G. Chen, X. Li, Ind. Eng. Chem. Res. 42 (2003) 653.

[30] M. Chatterjee, H. Hayashi, N. Saito, Micropor. Mesopor. Mater. 57 (2003) 143.
[31] L. Huang, J.C. Wu, S. Kawi, J. Mol. Catal. A 206 (2003) 371.
[32] M.J. Kim, R. Ryoo, Chem. Mater. 11 (1999) 487.
[33] Q. Huo, D.I. Margolese, G.D. Stucky, Chem. Mater. 8 (1996) 1147.
[34] J.S. Beck, J.C. Vartuli, W.J. Roth, M.E. Leonowicz, C.T. Kresge, K.D. Schmitt, C.T.-W. Chu, D.H. Olson, E.W. Sheppard, S.B. McCullen, J.B. Higgins, J.L. Schlenker, J. Am. Chem. Soc. 114 (1992) 10834.
[35] D. Kundu, H.S. Zhou, I. Honma, J. Mater. Sci. Lett. 17 (1998) 2089.
[36] T.S. Reighard, S.T. Lee, S.V. Olesik, Fluid Phase Equilib. 123 (1996) 215.